



http://pubs.acs.org/journal/acsodf Article

Spray-Deposited Rare Earth Metal Ion (Sm³⁺, Ce³⁺, Pr³⁺, La³⁺)-Doped CdO Thin Films for Enhanced Formaldehyde Gas Sensing Characteristics

Velusamy Periyasamy,* R. Ramesh Babu,* Awais Ahmad, Munirah D. Albaqami, Reham Ghazi Alotabi, and Elangovan Elamurugu*



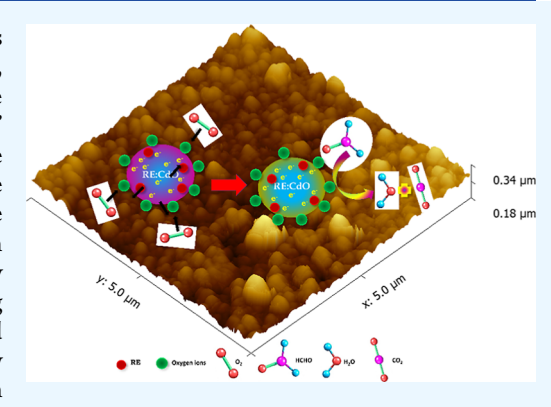
Cite This: ACS Omega 2022, 7, 35191-35203



ACCESS

Metrics & More

ABSTRACT: This study shows the electrical conductivity-dependent gas sensing characteristics of spray-deposited rare earth (RE) metal ion (Sm³+, Ce³+, Pr³+, La³+)-doped cadmium oxide (CdO) thin films on soda-lime microscope glass substrates at 300 °C. We examined the deposited films' structural, surface microstructural, DC electrical, and gas sensing features. The X-ray diffraction study indicates that all samples were polycrystalline, with the favored growth direction shifting from the (111) plane to the (200) plane. The highest root-mean-square values were obtained for the Pr-doped CdO thin film (5.86 nm). The surface microstructure of CdO thin films was significantly influenced by the RE metal ion dopant, with typical grain size values ranging from 64 nm to 134 nm depending on the dopant. The carrier concentration and resistivity of CdO films vary based on the RE metal ions used as dopants. Low resistivity (3.01 × 10^{-4} Ω .cm) was achieved for the CdO thin film doped with



Article Recommendations

La. High gas sensitivity (71.42%) was achieved for CdO thin films doped with La. The donor dopant regulated the electrical conductivity and gas sensing capabilities of CdO thin films.

1. INTRODUCTION

In recent years, with the advancement of modern industry and technology, the emission of numerous toxic gases has become a significant concern. Extensive research has been conducted on developing metal oxide semiconductor-based novel solidstate gas sensors. Consequently, the low-cost detection and quantification of gaseous species in air are becoming more important for health and safety, energy efficiency, and emission control.^{1,2} Consequently, considerable global interest is involved in inventing sensitive and selective gas sensors that are both dependable and efficient. Formaldehyde is one of the most extensively utilized volatile organic compound host materials in the chemical industry for producing construction materials and other home items.³ It is used in some fabrics, as a preservative in certain paints and coatings, and as an antiwrinkle agent in tiny doses.^{3,4} It is used extensively in the construction and furniture industries as a suitable adhesive. Long-term exposure to HCHO in the parts per billion level can induce chronic dermatitis, respiratory problems, leukemia, and sinus cancer. The World Health Organization's (WHO's) 30 min HCHO exposure limit is 0.08 ppm, but the Occupational Safety and Health Association's (OSHA1's) is 0.75 ppm time-weighted average (TWA). Due to the serious health risk, it is hard to make a sensitive HCHO gas sensor that can measure parts per billion-level HCHO in

indoor air. ^{1,6} Formaldehyde has been identified as the cause of cancer fatalities; current research indicates that manufacturing employees exposed to high quantities of formaldehyde have an increased chance of developing leukemia. ⁷ Therefore, finding formaldehyde in air is an essential and urgent matter from a practical point of view.

The semiconducting metal oxides (SMOs), including ZnO_s^{8-11} SnO_2 , $^{12-15}$ In_2O_3 , $^{16-19}$ and CdO_s^{20-23} offer excellent gas sensing characteristics because of their high chemical and thermal stability, surface morphology, and large surface-to-volume ratio. In recent years, several attempts have been made to enhance the sensitivity of SMO gas sensors, including modifying the morphology, adding different dopants, and developing semiconductor junctions. CdO thin films have been employed as sensing materials for ethanol, methional, acetone, toluene, 2-propanal, methane, and ammonia, among other analytes. 15,20,24 Recent papers on

Received: July 8, 2022 Accepted: September 12, 2022

Published: September 21, 2022





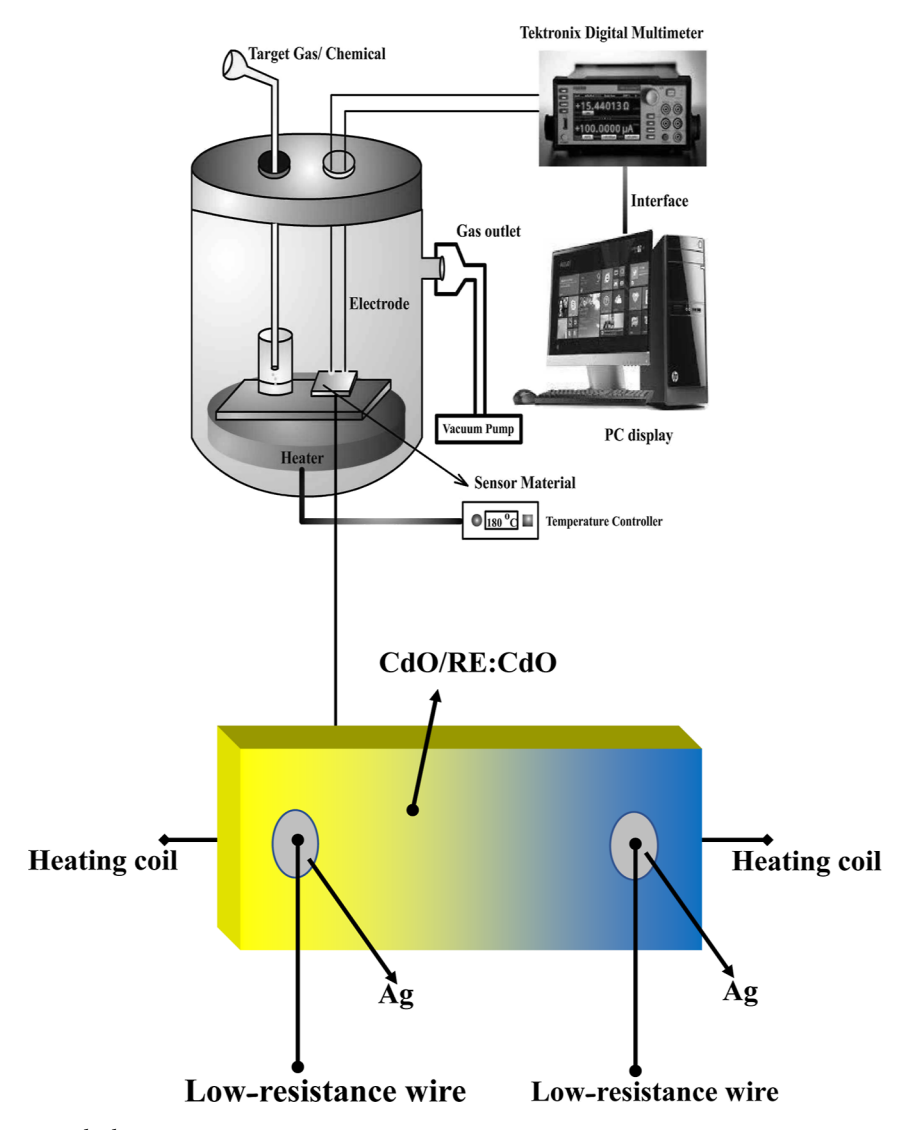


Figure 1. Measuring system with the sensor structure.

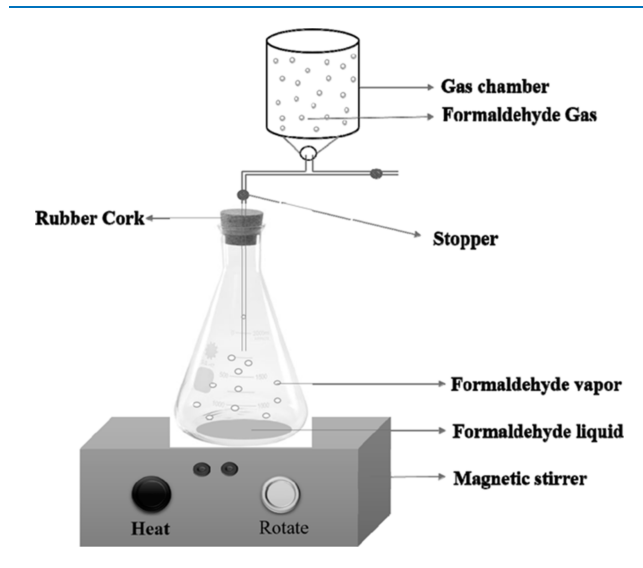


Figure 2. Schematic diagram of the formaldehyde vapor preparation system.

formaldehyde gas sensing explore the nature and mechanism of the response of metal oxide thin films, including SnO₂,

NiO, TiO_2 , and CdO-mixed In_2O_3 , for formaldehyde sensing. ^{16,24,24,25} Doping with sufficient metal ions may alter the starting materials' physical and chemical characteristics. However, there are few studies on metal ion-doped TCO thin films for formaldehyde gas detection. Wang et al.²⁶ found that a thin film of Pd-doped SnO₂ made with the sol-gel method had a maximum gas response of 0.03 ppm formaldehyde at 250 °C and a response and recovery time of 50 s. Tian et al. 10 revealed the selectivity features of a thin layer of Pb-doped SnO2. Kamble et al. reported a varied deposition timedependent ethanol gas reaction. 12 Sankarasubramanian et al. 28 studied the influence of the substrate temperature and Fedoping concentration on the ethanol gas reaction of CdO. Salunkhe et al.²⁰ investigated how the LPG gas reaction of CdO thin films changes with the temperature. Wang et al.²⁹ developed a SnO₂ hollow hexagonal prism HCHO gas sensor. SnO₂ hollow hexagonal prisms have a high response value and a quick reaction time to HCHO due to their high specific surface area. Meng et al.³⁰ described an HCHO gas sensor based on NiO-SnO₂ microflowers whose higher sensing performance was due to p-n heterojunctions and NiO's catalytic action. SMO-based gas sensors have progressed, but their poor sensitivity prevents real-time detection of parts per

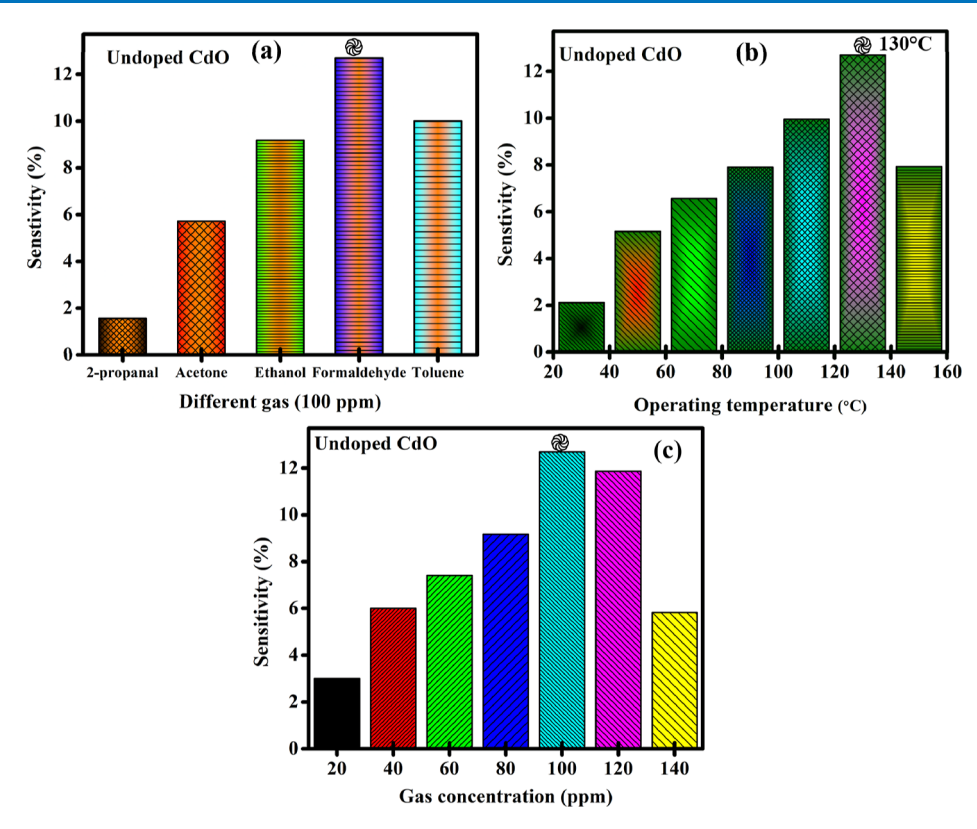


Figure 3. Gas sensing optimization processes of CdO thin films: (a) selectivity measurement, (b) sensor operating temperatures, and (c) gas concentrations.

billion-level HCHO. SMO-based gas sensors' sensitivity depends on the interaction between gas sensing materials and gas molecules. The number of collected target gas molecules is another critical component in determining the gas sensing transducing signal and sensitivity of the gas sensor. The sensitivity of a gas sensor will increase if more of the target gas is near the materials that detect it. 18,27,31

According to the literature studies, 16,17,21,24,28 dopants efficiently modify the optoelectronic and gas sensing capabilities of CdO thin films when the ionic radius or size of the dopant ions is slightly less or more or less equal to that of Cd²⁺ (0.097 nm). A few rare earth (RE) metal ions are used as dopants in the CdO lattice to modify the gas sensing capabilities in the current study. The effect of doping of RE metal ions (Sm³⁺, Ce³⁺, Pr³⁺, and La³⁺) on the structural, micromorphological, and optoelectronic characteristics of CdO thin films deposited by a simple chemical spray pyrolysis process has been described. 21,32-34 Presently, no electronic sensing is available for detecting formaldehyde gas, and there is no report on a formaldehyde gas sensor based on spraydeposited RE metal ion-doped CdO thin films. The effect of RE metal ion doping on the formaldehyde gas sensing properties of spray pyrolytically produced CdO thin films was investigated in this study using a simple and cost-effective chemical-resistance technique.

2. EXPERIMENTAL DETAILS

Preparation of undoped and RE metal ion-doped CdO thin films and their structural, microstructural, optical, and electrical characteristics are described in depth elsewhere. $^{21,32-34}$ All gas sensing studies were conducted at the optimal operating temperature of 130 $^{\circ}$ C.

2.1. Substances and Reagents. The analytical-grade cadmium acetate dihydrate (with 99.8% purity) was purchased from Merck. 99.95% purity precursors of samarium, lanthanum, cerium, and praseodymium(III) chloride hexahydrate were acquired from Sigma-Aldrich. For substrates and solvents, respectively, Lab-tech microscopic glass slides and Merck's 99.9% pure methanol were utilized. All chemical reagents were utilized without further purification.

2.2. Film Preparation. Undoped and RE-doped CdO thin films were deposited on $20 \times 20 \times 1.2 \text{ mm}^3$ microscopic glass slides preheated to 300 °C.35 The precursor solution comprised varying quantities of 0.05 M cadmium acetate dihydrate [Cd (CH₃COO)₂·2H₂O] and various wt % of RE metal ions. The distance between the substrate and the nozzle was fixed at 30 cm for all tests. The spray gun was held at a 45° angle and compressed, and filtered air at a constant pressure of 45 kg/cm² (44.13 bar) was employed as the carrier gas. The substrate temperature was regulated with an accuracy of 5 °C using a chrome-alumni thermocouple coupled to a digital temperature controller. The optimal deposition settings were maintained throughout the whole deposition procedure. When tiny droplets of the sprayed solution meet with heated glass substrates, pyrolytic decomposition occurs on the surface of the substrate, resulting in yellow CdO thin films with a uniform thickness.

2.3. Characterization Methods. The crystal system was validated using a PANalytical Empyrean X-ray diffractometer (Cu K1-1.5406). The thickness of the film was determined using an optical reflection technique (Filmetrics, Model: F20-XT). Surface roughness was evaluated using an atomic force microscope, and surface microstructures were investigated using a FEI NovaNano field emission scanning electron microscope. The electrical characteristics were measured using

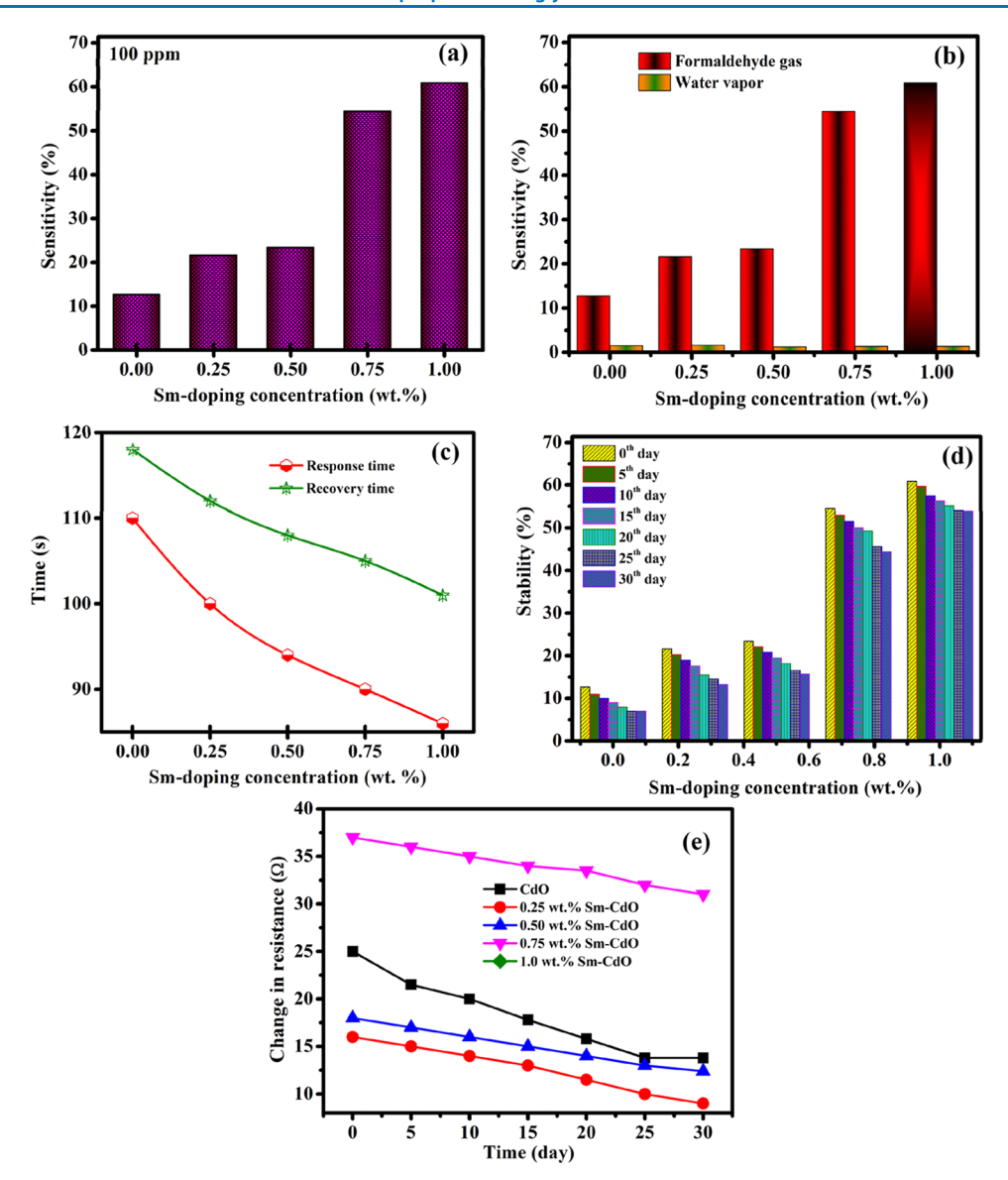


Figure 4. Formaldehyde gas sensing properties of Sm-doped thin films: (a) gas sensitivity, (b) water concentration in gas response, (c) response and recovery times, (d) resistance variation, and (e) sensor stability.

a van der Pauw configuration hall measuring setup (Ecopia, HMS 3000).

Figure 1 shows the experimental setup and sensor construction employed in this investigation and the electrode combinations. For gas sensing investigations, undoped and RE metal ion-doped CdO thin films were produced on glass substrates, and 1.0 mm thick Ag electrodes were grown on the substrate, with a 5.0 mm gap between the electrodes (Figure 1). The active area of the sensor material was 1 cm². The gastesting chamber (1.0 L capacity) was made of stainless steel with double walls. The sensor materials were placed on a hotplate that could be heated to 130 °C using the Eurotherm-2404 PID temperature controller (2 °C). Air was used as the carrier gas, while formaldehyde (HCOH) was used as the test gas. The sensor's response to exposure to the target gas was recorded as a change in resistance (Agilent 34401) using datagathering software. Thin films of undoped and RE-doped CdO were subjected to HCHO at varying temperatures and concentrations. As seen in Figure 2, the sample gas was generated using a basic improvised experimental apparatus.

Approximately 37% of the analytical gas (formaldehyde) was pure. The response and recovery times are the duration it takes for the sensor materials to reach their maximum resistance, followed by the period it takes for those values to return to their minimum. The gas response is the signal change per analyte concentration unit. The gas response of CdO thin films was determined using the relationship¹ below.

$$S \% = \frac{R_{\rm a} - R_{\rm g}}{R_{\rm g}} \times 100 \tag{1}$$

where S is the gas response, $R_{\rm a}$ is the sensor material's resistance in air, and $R_{\rm g}$ is the sensor material's (CdO film) resistance in gas.

Common SMOs-based gas sensors detect a gas and its impact on the electrical signal. Gas sensing mechanisms explain why gas modifies a sensor's electrical properties. We classify gas sensing mechanisms into two types. ¹⁵ One category analyzes electrical property changes from a microscopic standpoint using theories like Fermi level control, grain boundary barrier control, and electrical double layer (EDL)/

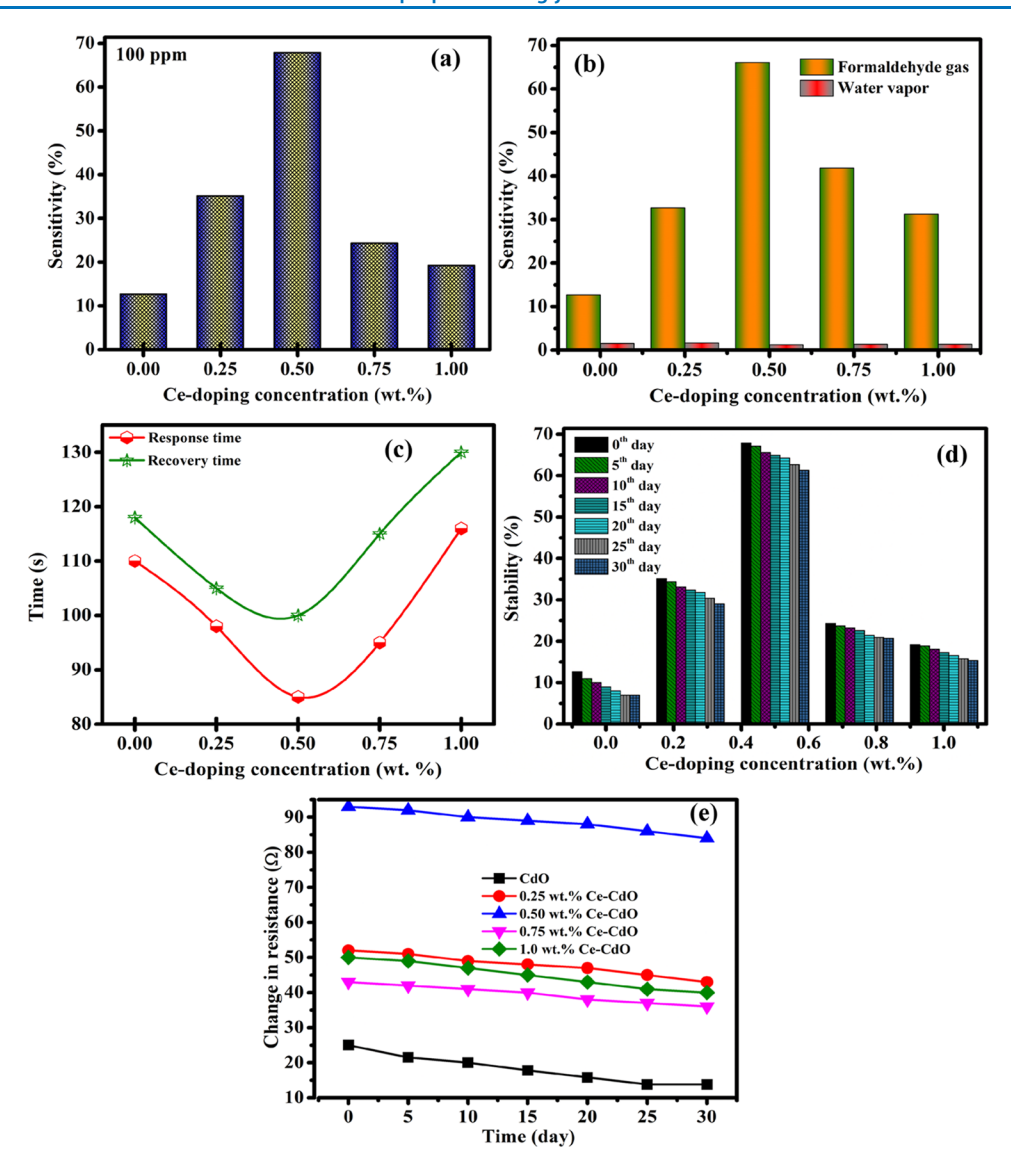


Figure 5. (a) Gas sensitivity, (b) water concentration in gas response, (c) response and recovery times, (d) resistance variability, and (e) sensor stability of Ce-doped thin films.

hole accumulation layer (HAL). Changes always follow changes in electrical properties in physical qualities like energy bands and work functions. Another theory is macroscopic and focuses on materials and gases. This theory includes adsorption/desorption, bulk resistance, and gas diffusion. These adsorption/desorption modes comprised three more models such as oxygen adsorption, chemical adsorption/desorption, and physical adsorption/desorption models. The oxygen adsorption model is the most popular gas sensing mechanism, and EDL and HAL are extensions of it. 36,37 When exposed to air, MOS adsorbed oxygen molecules. For n-type MOSs, we analyzed SnO₂. Li et al.³⁶ fabricated a simple integrated device using nanosheet-assembled hierarchical SnO₂ nanostructures. At high temperatures and in reducing environments, the surface of SnO₂ acted as a highly doped semiconductor with oxygen vacancies.

Thin metal oxide semiconductor films may detect a formaldehyde molecule by the adsorption and desorption of oxygen on the sensor's surface, which alters the sensor's resistance. Due to the greater electronegativity of the oxygen atom, when metal oxide semiconductor films are exposed to

air, oxygen molecules absorb electrons from the metal oxide semiconductor surface states at high temperatures and adsorb on the surface of the films. 27,27 Chemosorbed oxygen molecules undergo a delocalized charge transfer, resulting in a significant band bending and a change in the electrostatic potential toward the surface. The temperature has a role in the adsorption of oxygen molecules on the semiconductor surface. The temperature is crucial because the types of oxygen species that can be chemisorbed $\left(\mathrm{O_2}^-,\,\mathrm{O}^-,\,\mathrm{and}\,\mathrm{O}^{2-}\right)$ have discrete activation energies 6,15

$$O_{2(g)} \leftarrow \rightarrow O_{2(ads)}$$
 (2)

$$O_{2(ads)} + e^- \leftarrow \rightarrow O_{2(ads)}^-$$
 (3)

$$O_{2(ads)}^{-} + e^{-} \leftarrow \rightarrow 2O_{(ads)}^{-}$$
 (4)

$$O_{(ads)}^{-} + e^{-} \leftarrow \rightarrow O_{(ads)}^{2-}$$
 (5)

If formaldehyde is present in air, it reacts with air molecules by disporting oxygen, and the processes are summarized as follows^{1,35}

$$HCHO_{ads} + O_{(ads)}^{-} \Rightarrow CO_2 + H_2O + e^{-}$$
(6)

$$HCHO_{ads} + O_{2(ads)}^{-} \Rightarrow CO_2 + H_2O + 2e^{-}$$
 (7)

$$HCHO_{ads} + O_{(ads)}^{2-} \Rightarrow CO_2 + H_2O + 2e^-$$
 (8)

3. RESULTS AND DISCUSSION

3.1. Optimization of Gas Sensing Processes. In the current work, different gases, gas concentrations, and operating temperatures were optimized to achieve high gas sensitivity in CdO thin films produced by spray pyrolysis, as shown in Figure 3a-c. Figure 3a shows the gas sensitivity of an undoped CdO thin film as a function of analytic gases, including 2-propanal, acetone, ethanol, formaldehyde, and toluene. Formaldehyde has the highest sensitivity, at approximately 12.69%, and the quickest reaction and recovery durations among the numerous analytical gases. In order to achieve a high gas sensitivity, the working temperature was varied from room temperature to 150 °C, such as 30, 50, 70, 90, 110, 130, and 150 °C. At an operating temperature of 130 °C, significant gas sensitivity and rapid reaction and recovery were achieved (Figure 3b). We observed (Figure 3b) a progressive rise in gas sensitivity with increasing analytical (formaldehyde) gas concentration up to 100 ppm, followed by a reduction with increasing gas concentration. The CdO thin film shows remarkable gas sensitivity at 100 ppm formaldehyde gas concentration. In addition, the reaction and recovery periods increase steadily as the gas concentrations increases (Figure 3c). Formaldehyde is a good analytical gas for CdO thin films. An operating temperature of 130 °C and a gas concentration of 100 ppm are ideal for high gas sensitivity and good response and recovery times.

3.2. Gas Sensing Properties of RE-Doped CdO Thin Films. 3.2.1. Sm-Doped CdO Thin Films. The gas sensing behavior of Sm-doped CdO thin films is shown in Figure 4ae; it clearly shows that the gas response gradually increases with the Sm-doping concentration. The maximum gas response is 60.91% for the Sm-doped CdO thin film at 1.0 wt %, with response and recovery times of 86 and 101 s, respectively (Figure 4b,c). In addition, the influence of the water concentration on the formaldehyde reaction at an operating temperature of 130 °C was determined. The gas response values (for 100 ppm formaldehyde gas and water) are shown in Figure 4b, revealing that the water response is significantly smaller (1%) than the formaldehyde response. In the present investigation, the influence of water on the HCHO reaction was deemed minimal. The calculated values of gas response, recovery, and response times are given in Table 1. The fluctuation in resistance and long-term stability of undoped and Sm-doped CdO thin films is shown in Figure 4d,e, respectively. These results demonstrate that the reactions are reproducible to the same magnitude and have a stable baseline and resistance variation. 11 The resistance change of sensor materials is summarized in Table 1. In this instance, the concentration of free charge carriers considerably influences the resistance change of CdO thin films. Therefore, a thin CdO film doped with 1.0% Sm has a higher concentration of free carriers, which could cause a significant change in resistance during chemical absorption processes.

3.2.2. Ce-Doped CdO Thin Films. The calculated gas response of Ce-doped CdO thin films and the response time and recovery time are shown in Figure 5a,c, and Table 1. The

Table 1. Gas Sensing Properties of Undoped and RE-Doped CdO Thin Films

samples	Sm- doped CdO (wt %)	sensitivity (%)	response time (s)	recovery time (s)	change in resistance $R_{\rm c} \; (\Omega)$
Sm-doped CdO	0.00	12.69	110	118	25
	0.25	21.62	100	112	16
	0.50	23.37	94	108	18
	0.75	54.44	90	105	37
	1.00	60.91	86	101	53
Ce-doped CdO	0.00	12.69	110	118	25
	0.25	35.13	98	105	52
	0.50	67.88	85	100	93
	0.75	24.29	95	115	43
	1.00	19.23	116	130	50
Pr-doped CdO	0.00	12.69	110	118	25
	0.25	32.65	80	102	16
	0.50	66.10	65	86	39
	0.75	41.83	92	110	41
	1.00	31.25	120	140	25
La-doped CdO	0.00	12.69	110	118	25
	0.25	17.50	95	110	28
	0.50	43.93	89	105	29
	0.75	57.83	85	101	96
	1.00	71.42	80	97	50

0.5 wt % Ce-doped CdO thin film has the highest gas response of 67.88 and response and recovery times of 85 and 100 s, respectively (Figure 5a,c). The gas response gradually increases with increasing Ce-doping concentrations up to 0.50 wt % and then decreases for higher doping concentrations (0.75 and 1.0 wt %) (Table 1). Water concentration's influence on the formaldehyde reaction at 130 °C was also examined. Figure 5b shows the gas reaction (for 100 ppm formaldehyde gas and water), which is smaller (1%) than formaldehyde. In the present investigation, water's influence on the HCHO reaction was minimal. Figure 5d,e shows the variation in resistance and long-time stability of undoped and Ce-doped CdO thin films, respectively. Results are consistent in the magnitude and have strong baseline stability and resistance fluctuation as shown by these graphs. 16 The change in resistance is summarized in Table 1.

3.2.3. Pr-Doped CdO Thin Films. Figure 6a-e shows the results of experiments in which the influence of gas sensing behavior of undoped and Pr-doped CdO thin films was measured. The computed gas response of Pr-doped CdO thin films and the response time and recovery time are shown in Figure 6a,c, and the results are further summarized in Table 1. The Pr-doped CdO thin film with a concentration of 0.5 wt % has the most significant gas response of 66.10%, and its response and recovery times are, respectively, 65 and 86 s (Figure 6a,c). The gas reaction increases up to a point when the Pr-doping concentration is 0.50 wt %, and then, it begins to decline as the doping concentration increases to 0.75 and 1.0 wt % (Table 1). At a temperature of 130 °C, the impact of the water vapor concentration on the formaldehyde reaction was also investigated. Figure 6b shows the gas reaction, which is much less significant (1%) than the formaldehyde reaction. In the current experiment, water vapor's impact on the

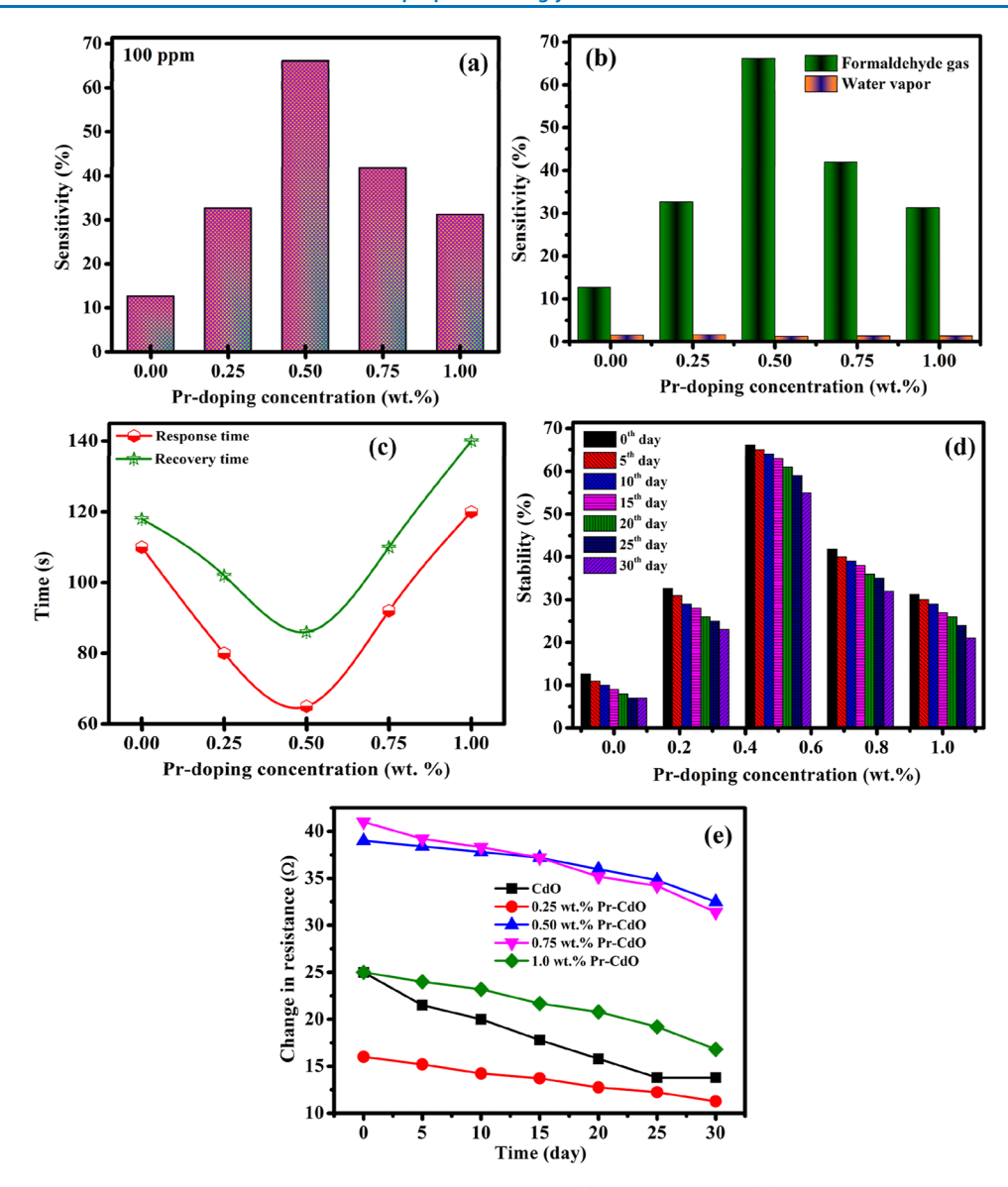


Figure 6. Pr-doped CdO thin films' formaldehyde gas detecting properties: (a) gas sensitivity, (b) water concentration in gas response, (c) response and recovery times, (d) resistance change, and (e) sensor stability.

HCHO reaction was negligible (Figure 6b). The change in resistance and long-term stability of undoped and Pr-doped CdO thin films is shown, respectively, in Figure 6d,e. As seen in these figures,²⁴ the results are reliable in terms of size and exhibit high levels of baseline stability and resistance fluctuation. Table 1 provides a summary of the changes in resistance that have taken place.

3.2.4. La-Doped CdO Thin Films. Figure 7a—e shows the gas sensing characteristics of undoped and La-doped CdO thin films. Figure 7a,c shows the calculated gas response of La-doped CdO thin films, and Table 1 summarizes the findings. La-doped CdO thin film with a 1.0 wt % concentration had the highest gas response (71.42%) and response and recovery periods (80 and 97 s, respectively) (Figure 7a,c). The reactivity of CdO thin films to formaldehyde gas steadily rises with increasing La-doping concentration (Table 1). At 130 °C, the influence of the water vapor concentration on formaldehyde reaction was also studied. Figure 6b shows the gas response, which is less substantial (1%). In this experiment, water vapor did not affect the HCHO reaction

(Figure 7b). Figure 7d,e shows the long-term resistance and stability of undoped and La-doped CdO thin films. The figure shows that the findings depend on the size, baseline stability, and resistance fluctuation. ²⁷Table 1 shows resistance changes.

3.2.5. Gas Sensing Mechanism. A gas sensor's sensitivity and response time are directly linked to the target gas's diffusion rates and surface reactions. The microstructure and size of target gas molecules restrict gas diffusion, whereas the surface reaction rate is influenced by the sensor layer's catalytic activity and operating temperature.²⁹ The response time of gas sensors is primarily determined by the period at which diffusion and surface reaction reach equilibrium.^{29,30} For semiconductor gas sensors, the gas diffusion and surface reaction are critical characteristics. Based on the gas adsorption-induced charge transfer phenomena, the HCHO gas sensing mechanism of current materials may be described (Figure 8). Upon exposing the gas sensor to air, oxygen molecules are adsorbed on its surface and transformed into chemisorbed oxygen species (O_{2ads}-, O_{ads}-, and O_{ads}²⁻) by acquiring electrons from its conduction band.³¹ Consequently,

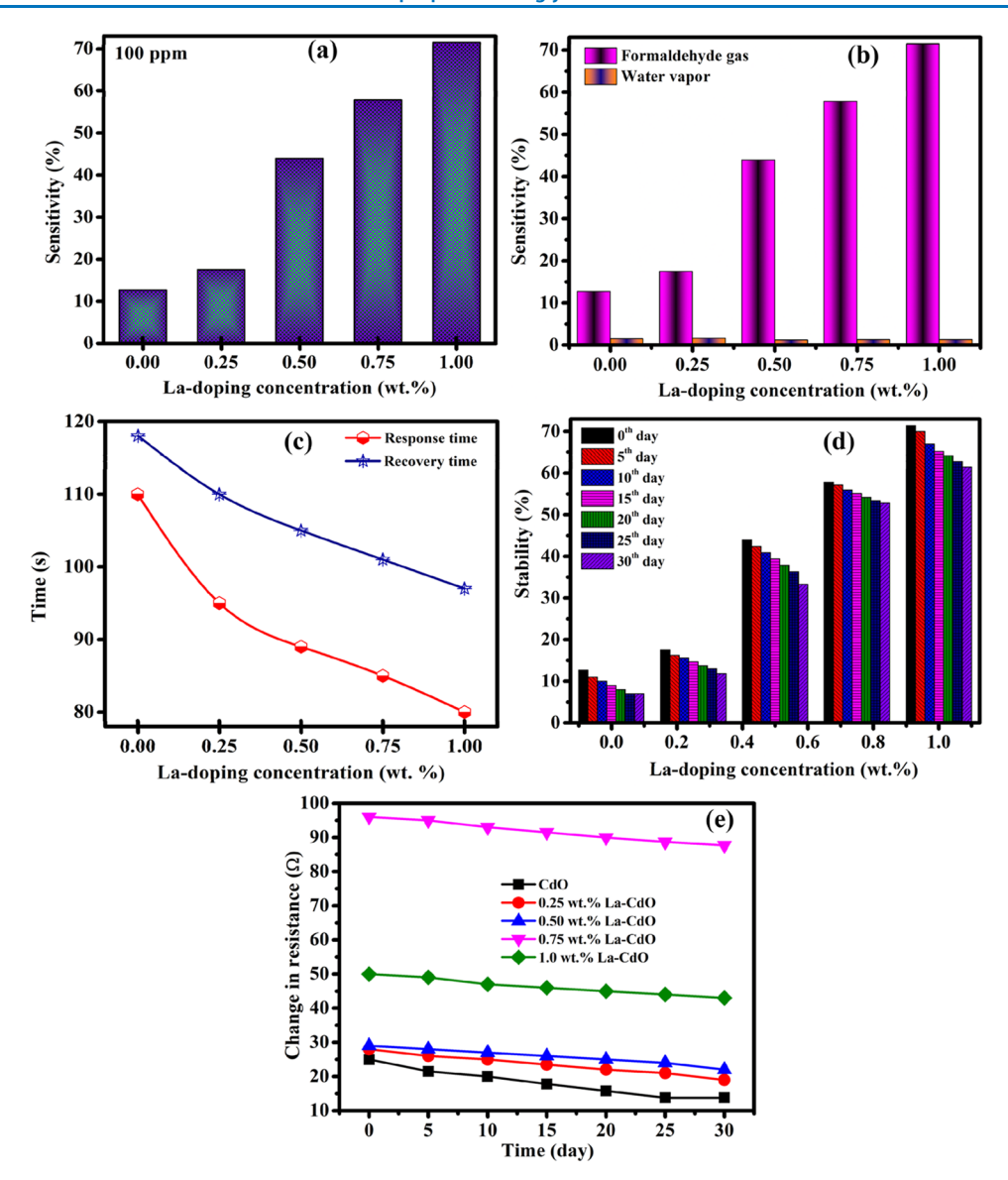


Figure 7. La-doped CdO thin films' formaldehyde gas detecting characteristics: (a) gas sensitivity, (b) water concentration in gas response, (c) response and recovery times, (d) resistance change, and (e) sensor stability.

the electron density in the detecting layer of a gas sensor decreases, leading to a thicker depletion layer. Electrons constitute the bulk of charge carriers in an n-type semiconductor (CdO and RE-doped CdO thin films). Upon exposing the gas sensor to reducing (electron-donating) gases such as HCHO, chemisorbed oxygen species react with HCHO and release electrons back into the sensor's depletion layer. Consequently, the gas sensor's resistance decreases. 5,38

Generally, RE ions have an empty 4f level; thus, they add more electrons to the conduction band of CdO, increasing electrical conductivity, which may aid in improving gas sensitivity. Cd²⁺ has an ionic radius of 0.096 nm, whereas Sm³⁺, Ce³⁺, Pr³⁺, and La³⁺ have an ionic radius of 0.095, 0.101, 0.099, and 0.103 nm, respectively. Because the ionic radius of RE ions is so close to that of Cd²⁺, the substitution most certainly occurs, increasing the amount of conduction band electrons. RE dopants reduce the reaction activation energy between the target gas and surface-adsorbed oxygen, resulting in improved sensing responsiveness to target gases. It is well documented in the literature that RE metal doping

reduces the optimal working temperature of metal oxides and renders a sensor selective to a particular gas. The gas sensitivity of RE-doped CdO thin films increases progressively with RE-doping concentrations, probably due to a gradual increase in free charge carrier concentrations. Increasing the carrier concentration may result in substituting Cd²⁺ with RE³⁺, in which RE³⁺ functions as a donor impurity and offers one extra free electron at the lowest conduction band level.

Furthermore, because O_{2ads} quickly recognizes these free electrons and O_{2ads} , the number of free charge carriers decreases, increasing the resistivity and conductivity of the CdO thin film. The sensitivity of the La³⁺-doped CdO thin film is the highest among all the RE metal ion-doped CdO thin films. According to the findings of this investigation, all CdO thin films doped with RE ions are suitable for use as formaldehyde gas sensors. At ambient temperature, the surface of metal oxide semiconductor (CdO thin films) thin films is generally populated with physisorbed and chemisorbed species such as O^{-2} , OH^- , and H_2O . At temperatures above $100\,^{\circ}$ C, the ions O^- and O^2 -predominate. In our research, the

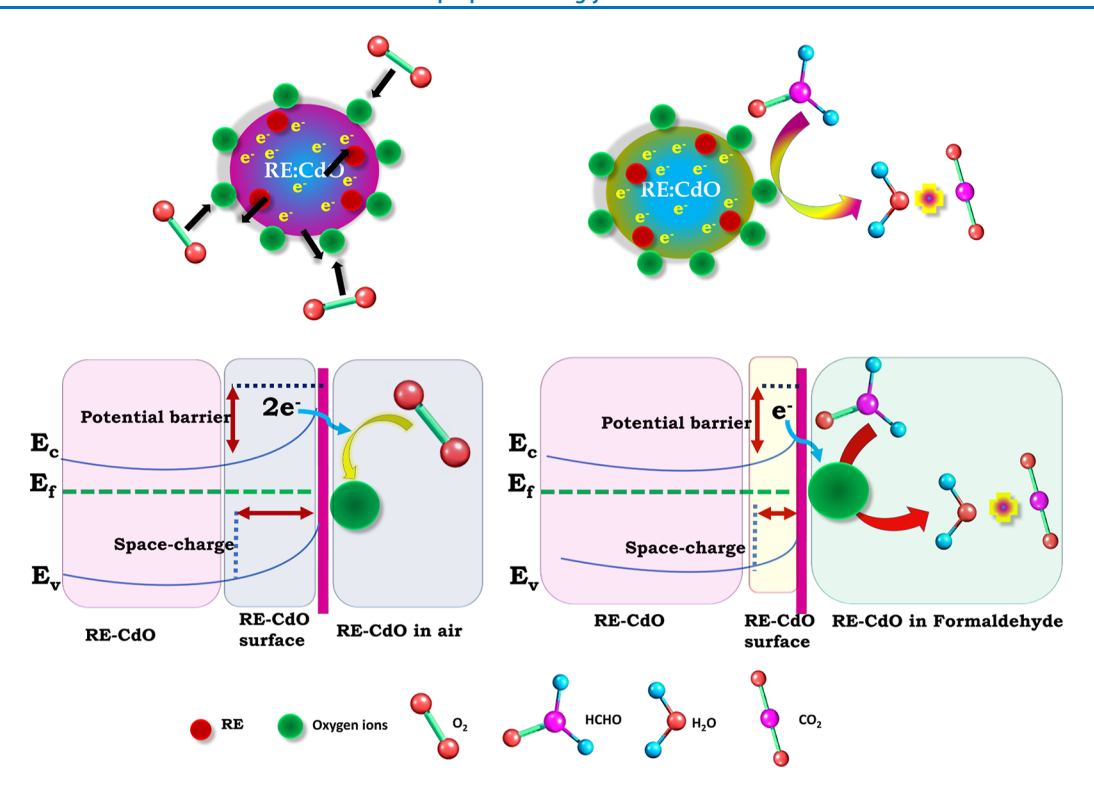


Figure 8. Schematic illustration of the formaldehyde gas sensing mechanism for RE-doped CdO thin films with the possible gas sensing reaction and electron transfer in air and gas sensing reaction and electron transfer in formaldehyde vapors.

excellent sensor responses may be attributed to the responses (eqs 2 and 3) when the operating temperature surpasses 120 $^{\circ}\text{C.}^{39,40}$

When the sensor is exposed to formaldehyde gas, the adsorbed oxygen ions O_{ads} (O_{2ads} , O_{ads} , O_{ads}) are created on the CdO surface to produce CO2 and H2O. As the electron concentration rises, the trapped electrons rapidly return to the CdO conduction band, providing the surface depletion layer, lower potential barrier, and reduced resistance.^{27,38} The sensor has good formaldehyde gas sensing capability for two reasons (Figure 8). RE-doped CdO thin films are generated from many small particles or crystals. This shape enhances the sensor's specific surface area, which facilitates the adsorption of gas molecules on RE-doped CdO thin films and the diffusion of formaldehyde gas, speeding the sensor's reaction rate. Doping RE may add oxygen adsorption sites. Once formaldehyde contacts the sensor, the RE metal may oxidize. This action may create more electrons, rapidly returning to CdO's conduction band, decreasing the sensor's resistance. 30,39 Also, sensor gas responsiveness improves when the grain size is double the electron depletion layer thickness. It enhances the formaldehyde gas-adsorbed cation reaction and the sensor's gas sensing capability. The increased formaldehyde responses are due to the unique surface structure, RE-doping, high crystalline quality, and sufficient surface adsorption sites.

3.3. X-ray Diffraction Analysis. Figure 9 shows the structural characteristics of undoped and different RE metal ion-doped CdO thin films. The observed diffraction peaks correspond closely to the reference data. From Figure 9, it can be seen that the undoped CdO film grows preferentially along the (111) plane. All RE (1.0 wt % Sm³⁺, 0.50 wt %-Ce³⁺, 0.50 wt %-Pr³⁺, and 1.0 wt %-La³⁺)-doped CdO thin films exhibited a change in the growth direction from the (111)

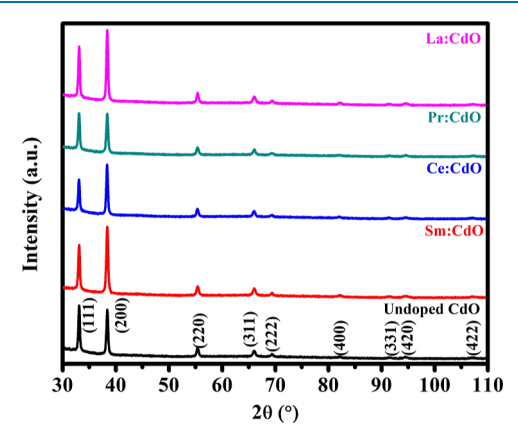


Figure 9. XRD pattern of undoped and Sm³⁺-, Ce³⁺-, Pr³⁺-, and La³⁺-doped CdO thin films.

plane to the (200) plane.^{21,32–34} In Sm- and La-doped CdO thin films, the intensity of the (200) plane is more significant than in Ce- and Pr-doped CdO thin films. This change is most likely a result of the integration of the RE dopant into the CdO lattice. Table 2 summarizes the estimated average crystallite size (D) from the (200) plane using Scherrer's formula.³⁵ It was discovered that the crystallite size varied with the RE doping concentration. Table 2 provides a summary of the computed microstrain and dislocation density. Crystallization processes in polycrystalline thin films may alter the microstrain and dislocation density of CdO thin films as well as the composition of the dopants. These modifications may contribute to the gas sensing capabilities of CdO thin films.

3.5. AFM Analysis. Figure 10a—e shows the three-dimensional surface topography recorded using atomic force microscopy (AFM); the section $(0.5 \ \mu m \times 0.5 \ \mu m)$ is utilized

Table 2. Structural Parameters Evaluated from XRD Data for RE-Doped CdO Thin Films

plane	doping concentration (Ti) (wt %)	"a" (Å)	"D" (nm)	$(10^{14} \text{Lines/m}^2)$	"ε" (10 ⁻³)
(200)					
	0.00	4.691	21	2.35	1.68
	1.0 wt % Sm	4.690	23	1.88	1.50
	0.5 wt % Ce	4.693	26	1.39	1.29
	0.5 wt % Pr	4.690	25	1.55	1.38
	1.0 wt % La	4.691	25	1.68	1.60

for measuring the surface roughness. A root-mean-square (RMS) roughness of 2.24 nm was estimated for the undoped CdO film (Table 3). The RMS value varies for various RE-doped CdO; for 1.0 wt % Sm-doped CdO, it is 2.42 nm, 2.96 nm for 0.5 wt % Ce-doped CdO, 5.86 nm for 0.5 wt % Pr-doped CdO, and 5.38 nm for 1.0 wt % La-doped CdO. It is important to note that several adhering particles generate the

unusual surface structure of CdO. Because their typical size is near their Debye radius, these microscopic particles may serve as conductive switches if all electrons are depleted. In addition, these particles may provide several adsorption sites (Figures 10 and 11), improving the sensor's sensitivity.³⁸ The increasing surface roughness with introducing various RE dopants is associated with the increasing grain size of CdO thin films. The variation in the RE dopant influenced the variation in surface roughness.⁴¹

3.6. FE-SEM Analysis. The field-emission scanning electron microscopy (FE-SEM) images of undoped and RE (1.0 wt % Sm³⁺, 0.50 wt %-Ce³⁺, 0.50 wt %-Pr³⁺, and 1.0 wt %-La³⁺)-doped CdO thin films are compared in Figure 11a—e as a function of the RE dopant to determine the influence of the RE dopant on the surface micromorphology. According to the FE-SEM microstructures, the as-deposited (Figure 11a) films are densely packed with spherical-shaped agglomerated grains. Figure 11b shows that the surface microstructure of 1.0 wt % Sm-doped CdO thin films comprised increased

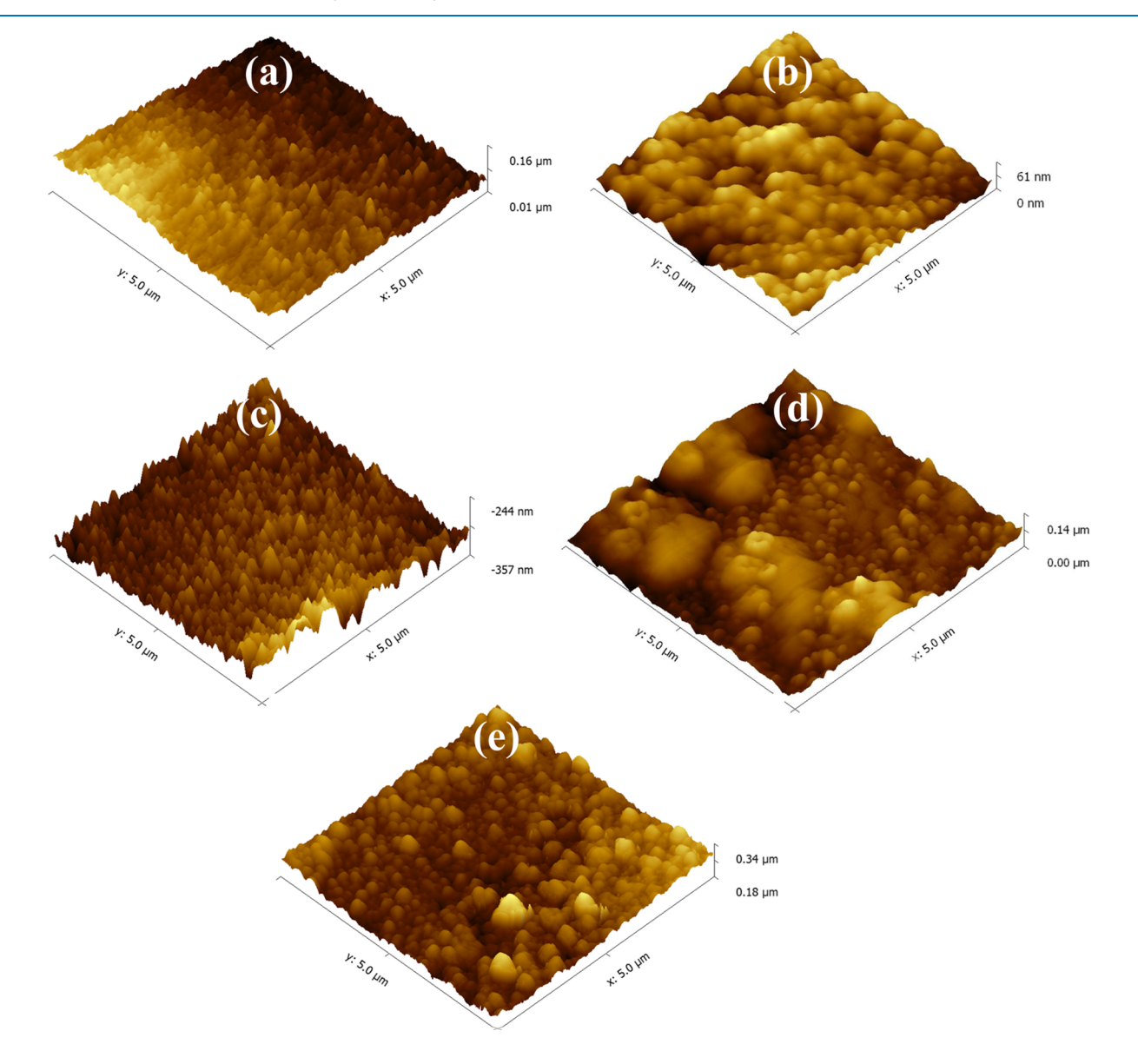


Figure 10. Surface topography (AFM) of RE-doped CdO thin films: (a) undoped CdO, (b) 1.0 wt % Sm-doped, (c) 0.5 wt % Ce-doped, (d) 0.5 wt % Pr-doped, and (e) 1.0 wt % La-doped CdO thin films.

Table 3. Comparison of the RMS Values, Average Grain Size, and Electrical Parameters as a Function of RE-Doped CdO Thin Films

doped CdO wt % (RE)	RMS (nm) (AFM)	"d" (FE-SEM (nm))	$n_e \ (10^{20}/cm^3)$	$\mu_{\rm e}~({ m cm^2/Vs})$	$ ho~(10^{-4}~\Omega\cdot\mathrm{m})$	$\sigma~(10^3/\Omega\cdot\mathrm{cm})$
CdO	2.24	64	1.01	68	9.32	1.07
1.0 wt % Sm	2.12	65	4.05	45	3.36	2.45
0.5 wt % Ce	2.96	134	3.85	40	3.81	2.62
0.5 wt % Pr	5.86	145	2.19	82	3.49	2.86
1.0 wt % La	5.38	95	4.10	52	3.01	3.40

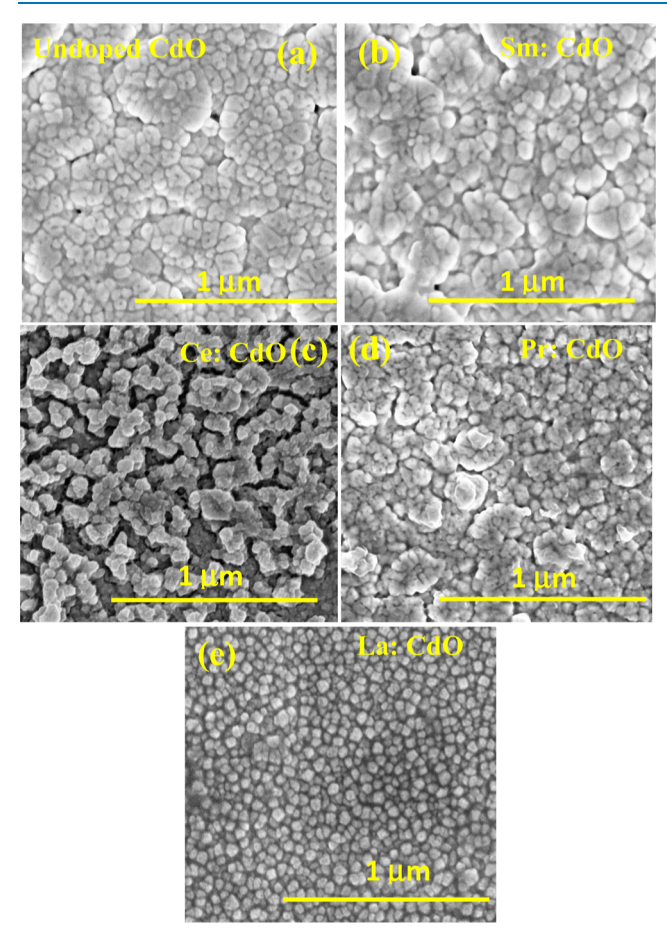


Figure 11. Surface microstructure (FE-SEM): (a) undoped CdO, (b) 1.0 wt % Sm-doped, (c) 0.5 wt % Ce-doped, (d) 0.5 wt % Pr-doped, and (e) 1.0 wt % La-doped CdO thin films.

spherical-shaped grains and a few patches. The 0.50 wt % Cedoped CdO (Figure 11c) film reveals that the grains are spherical and equally dispersed throughout the substrate surface with more patches. As the doping level of the 0.50 wt % Pr-doped CdO thin film increases, the grain size and shape change (Figure 11d). The surface of the film in Figure 11e appears to include uniformly dispersed spherical-shaped smiles devoid of pinholes and agglomeration. The average particle size (d) of CdO thin films increased as a function of RE dopant (64 nm for pure CdO, 80 nm for Sm-doped, 84 nm for Ce-doped, 92 for Pr-doped, and 114 nm for La-doped CdO thin films), indicating that the La-doped CdO thin film has improved crystallinity and plays a significant role in gas sensing processes. Therefore, the La-doped CdO thin film has greater gas sensitivity than undoped and other RE-doped CdO thin films.

3.7. Electrical Properties. At ambient temperature, the electrical characteristics of undoped and RE (1.0 wt % Sm3+, 0.5 wt % Ce3+, 0.50 wt % Pr3+, and 1.0 wt % La 3+)-doped CdO thin films were measured using the usual van der Pauw configuration. The measured values are summarized in Table 3 and shown in Figure 12a,b. Hall measurements demonstrate that CdO films are highly conducting n-type conductors. The high carrier concentration $(4.10 \times 10^{20} \text{ cm}^{-3})$ is attained for La-doped CdO thin films. Among the various RE dopants, Prdoped CdO thin films with a high carrier concentration, low resistivity, and high conductivity have the maximum electron mobility (85 cm²/V. s). The increase in charge carrier concentration can be attributed to the substitution of RE (Sm³⁺, Ce³⁺, Pr³⁺, La³⁺) ions with Cd²⁺ in the CdO lattice, which will result in more free electrons in the conduction band of CdO, hence increasing the material's conductivity. Because more free electrons are involved in the surface chemical reaction during the sensing processes, 23,33 increasing charge carrier concentration plays a significant role in

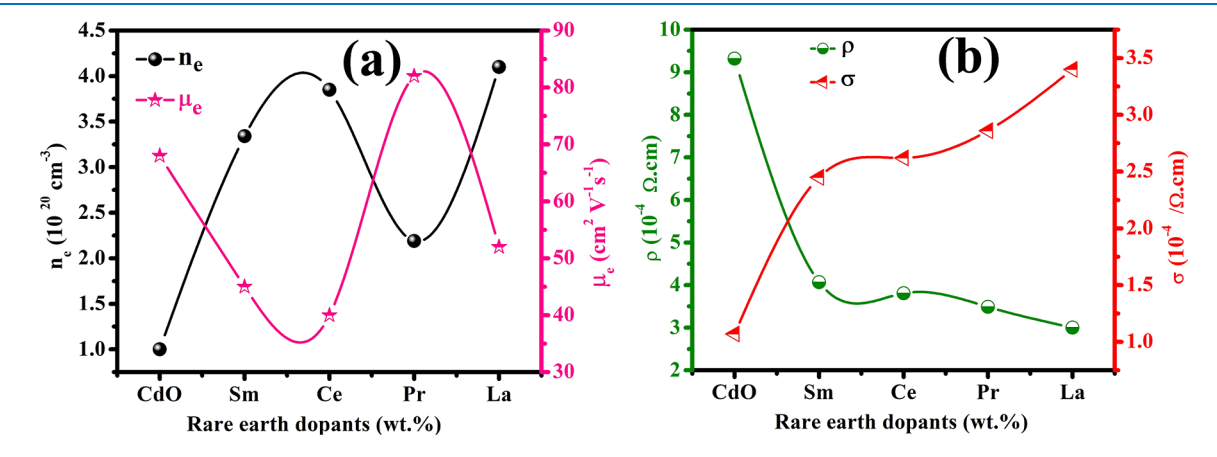


Figure 12. Electrical properties of the sensor: (a) carrier concentration, (b) electron mobility, (c) resistivity, and (d) conductivity undoped and Sm³⁺-, Ce³⁺-, Pr³⁺-, and La³⁺-doped CdO thin films.

enhancing the gas sensing characteristics of CdO thin films in this study.

4. CONCLUSIONS

The essential aspects and features of gas sensors are explored. The sensing characteristics of spray-deposited undoped and several RE metal ion (Sm³⁺, Ce³⁺, Pr³⁺, La³⁺)-doped CdO thin films were effectively shown by utilizing the chem-resistive technique with formaldehyde gas as the analyte gas. Spraydeposited CdO is highly selective for formaldehyde over others (acetone, ethanol, 2-propanal, and toluene) and sensitive to formaldehyde (100 ppm) at an operating temperature of 130 °C. The maximum sensitivity of the Ladoped CdO thin film is around 71.42% when compared to other RE metal ion-doped CdO thin films. The X-ray diffraction (XRD) pattern demonstrates that the favored growth orientation of CdO thin films switched from the (111) plane to the (200) plane. The FE-SEM reveals that the RE dopants efficiently modified the surface microstructure and particle size of CdO thin films. A high electrical conductivity and concentration of electron charge carriers were obtained for La-doped CdO thin films. As concluded in the current study, the increased structural, morphological, and electrical characteristics of RE-doped CdO thin films confer excellent gas sensing properties, and RE metal ion-doped CdO thin films are ideal candidates for formaldehyde gas sensor applications.

AUTHOR INFORMATION

Corresponding Authors

Velusamy Periyasamy — Crystal Growth and Thin Film Laboratory, Department of Physics, Bharathidasan University, Tiruchirappalli 620 024 Tamil Nadu, India; Department of Physics, Thiagarajar College of Engineering, Madurai 625015 Tamil Nadu, India; orcid.org/0000-0002-3443-1146; Email: Velusamy.phy@gmail.com

R. Ramesh Babu — Crystal Growth and Thin Film Laboratory, Department of Physics, Bharathidasan University, Tiruchirappalli 620 024 Tamil Nadu, India; Email: rampap2k@yahoo.co.in

Elangovan Elamurugu – iDARE Laboratory, Department of Physics and Nanotechnology, College of Engineering and Technology, SRM Institute of Science and Technology, Kattankulathur 603 203 Tamilnadu, India; Email: eevan1972@gmail.com

Authors

Awais Ahmad — Departamento de Quimica Organica, Universidad de Cordoba, E14014 Cordoba, Spain Munirah D. Albaqami — Chemistry Department, College of Science, King Saud University, Riyadh 11451, Saudi Arabia Reham Ghazi Alotabi — Chemistry Department, College of Science, King Saud University, Riyadh 11451, Saudi Arabia

Complete contact information is available at: https://pubs.acs.org/10.1021/acsomega.2c04303

Notes

The authors declare no competing financial interest.

ACKNOWLEDGMENTS

This work was funded by the Researchers Supporting Project Number (RSP-2021/267) King Saud University, Riyadh, Saudi Arabia. The author P.V. thanks J.V. from Khalifa University for the XRD and SEM facilities and wonderful research discussion.

REFERENCES

- (1) Chung, P.-R.; Tzeng, C.-T.; Ke, M.-T.; Lee, C.-Y. Formaldehyde Gas Sensors: A Review. Sensors 2013, 13, 4468-4484.
- (2) Chen, D.; Yuan, Y. J. Thin-Film Sensors for Detection of Formaldehyde: A Review. *IEEE Sens. J.* **2015**, *15*, 6749–6760.
- (3) Godbole, R.; Godbole, V. P.; Alegaonkar, P. S.; Bhagwat, S. Effect of Film Thickness on Gas Sensing Properties of Sprayed WO3 Thin Films. *New J. Chem.* **2017**, *41*, 11807–11816.
- (4) Assili, K.; Gonzalez, O.; Alouani, K.; Vilanova, X. Structural, Morphological, Optical and Sensing Properties of SnSe and SnSe2 Thin Films as a Gas Sensing Material. *Arabian J. Chem.* **2020**, *13*, 1229–1246.
- (5) Zhu, L.; Wang, J.; Liu, J.; Xu, Z.; Nasir, M. S.; Chen, X.; Wang, Z.; Sun, S.; Ma, Q.; Liu, J.; Feng, J.; Liang, J.; Yan, W. In Situ Enrichment Amplification Strategy Enabling Highly Sensitive Formaldehyde Gas Sensor. *Sens. Actuators, B* **2022**, *354*, 131206.
- (6) Castro-Hurtado, I.; Mandayo, G. G.; Castaño, E. Conductometric Formaldehyde Gas Sensors. A Review: From Conventional Films to Nanostructured Materials. *Thin Solid Films* **2013**, *548*, 665–676
- (7) Yadav, A. A.; Lokhande, A. C.; Shinde, P. A.; Kim, J. H.; Lokhande, C. D. CO2 Gas Sensing Properties of La2O3 Thin Films Deposited at Various Substrate Temperatures. *J. Mater. Sci.: Mater. Electron.* **2017**, 28, 13112–13119.
- (8) Kasirajan, K.; Bruno Chandrasekar, L.; Maheswari, S.; Karunakaran, M.; Shunmuga Sundaram, P. A Comparative Study of Different Rare-Earth (Gd, Nd, and Sm) Metals Doped ZnO Thin Films and Its Room Temperature Ammonia Gas Sensor Activity: Synthesis, Characterization, and Investigation on the Impact of Dopant. *Opt. Mater.* **2021**, *121*, 111554.
- (9) David, S. P.; Veeralakshmi, S.; Nehru, S.; Kalaiselvam, S. A highly sensitive, selective and room temperature operatable formaldehyde gas sensor using chemiresistive g-C3N4/ZnO. *Mater. Adv.* **2020**, *1*, 2781–2788.
- (10) Tian, H.; Fan, H.; Li, M.; Ma, L. Zeolitic Imidazolate Framework Coated ZnO Nanorods as Molecular Sieving to Improve Selectivity of Formaldehyde Gas Sensor. *ACS Sens.* **2016**, *1*, 243–250.
- (11) Yang, Y.; Wu, S.; Cao, Y.; Li, S.; Xie, T.; Lin, Y.; Li, Z. A Highly Efficient Room-Temperature Formaldehyde Gas Sensor Based on a Ni-Doped ZnO Hierarchical Porous Structure Decorated with NiS Illuminated by UV Light. *J. Alloys Compd.* **2022**, 920, 165850
- (12) Kamble, D. L.; Harale, N. S.; Patil, V. L.; Patil, P. S.; Kadam, L. D. Characterization and NO2 Gas Sensing Properties of Spray Pyrolyzed SnO2 Thin Films. *J. Anal. Appl. Pyrolysis* **2017**, *127*, 38–46.
- (13) Chung, F.-C.; Wu, R.-J.; Cheng, F.-C. Fabrication of a Au@ SnO2 core-shell structure for gaseous formaldehyde sensing at room temperature. *Sens. Actuators, B* **2014**, *190*, 1–7.
- (14) Kang, Z.; Zhang, D.; Li, T.; Liu, X.; Song, X. Polydopamine-Modified SnO2 Nanofiber Composite Coated QCM Gas Sensor for High-Performance Formaldehyde Sensing. *Sens. Actuators, B* **2021**, 345, 130299.
- (15) Li, Y.; Chen, N.; Deng, D.; Xing, X.; Xiao, X.; Wang, Y. Formaldehyde Detection: SnO2 Microspheres for Formaldehyde Gas Sensor with High Sensitivity, Fast Response/Recovery and Good Selectivity. Sens. Actuators, B 2017, 238, 264–273.
- (16) Wang, X.; Zhang, J.; Wang, L.; Li, S.; Liu, L.; Su, C.; Liu, L. High Response Gas Sensors for Formaldehyde Based on Er-Doped In2O3 Nanotubes. *J. Mater. Sci. Technol.* **2015**, *31*, 1175–1180.
- (17) Wang, Z.; Hou, C.; De, Q.; Gu, F.; Han, D. One-Step Synthesis of Co-Doped In2O3 Nanorods for High Response of

- Formaldehyde Sensor at Low Temperature. ACS Sens. 2018, 3, 468–475.
- (18) Liu, J.; Zhang, L.; Cheng, B.; Fan, J.; Yu, J. A High-Response Formaldehyde Sensor Based on Fibrous Ag-ZnO/In2O3 with Multi-Level Heterojunctions. *J. Hazard. Mater.* **2021**, 413, 125352.
- (19) Bai, J.; Luo, Y.; Chen, C.; Deng, Y.; Cheng, X.; An, B.; Wang, Q.; Li, J.; Zhou, J.; Wang, Y.; Xie, E. Functionalization of 1D In2O3 Nanotubes with Abundant Oxygen Vacancies by Rare Earth Dopant for Ultra-High Sensitive Ethanol Detection. *Sens. Actuators, B* **2020**, 324, 128755.
- (20) Salunkhe, R. R.; Shinde, V. R.; Lokhande, C. D. Liquefied Petroleum Gas (LPG) Sensing Properties of Nanocrystalline CdO Thin Films Prepared by Chemical Route: Effect of Molarities of Precursor Solution. *Sens. Actuators, B* **2008**, *133*, 296–301.
- (21) Velusamy, P.; Babu, R. R.; Ramamurthi, K.; Viegas, J.; Elangovan, E. Structural, Microstructural, Optical and Electrical Properties of Spray Deposited Rare-Earth Metal (Sm) Ions Doped CdO Thin Films. J. Mater. Sci.: Mater. Electron. 2015, 26, 4152–4164
- (22) Chandiramouli, R.; Jeyaprakash, B. G. Operating Temperature Dependent Ethanol and Formaldehyde Detection of Spray Deposited Mixed CdO and MnO2 Thin Films. *RSC Adv.* **2015**, *5*, 43930–43940
- (23) Bhosale, C. H.; Kambale, A. V.; Kokate, A. V.; Rajpure, K. Y. Structural, Optical and Electrical Properties of Chemically Sprayed CdO Thin Films. *J. Mater. Sci. Eng. B* **2005**, *122*, 67–71.
- (24) Velusamy, P.; Babu, R. R.; Ramamurthi, K.; Elangovan, E.; Viegas, J.; Sridharan, M. Gas Sensing and Opto-Electronic Properties of Spray Deposited Cobalt Doped CdO Thin Films. *Sens. Actuators, B* **2018**, 255, 871–883.
- (25) Lin, S.; Li, D.; Wu, J.; Li, X.; Akbar, S. A. A Selective Room Temperature Formaldehyde Gas Sensor Using TiO2 Nanotube Arrays. Sens. Actuators, B 2011, 156, 505–509.
- (26) Wang, J.; Zhang, P.; Qi, J.-Q.; Yao, P.-J. Silicon-Based Micro-Gas Sensors for Detecting Formaldehyde. Sens. Actuators, B 2009, 136, 399–404
- (27) Li, G.; Fan, Y.; Hu, Q.; Zhang, D.; Ma, Z.; Cheng, Z.; Wang, X.; Xu, J. Morphology and Size Effect of Pd Nanocrystals on Formaldehyde and Hydrogen Sensing Performance of SnO2 Based Gas Sensor. J. Alloys Compd. 2022, 906, 163765.
- (28) Sankarasubramanian, K.; Soundarrajan, P.; Sethuraman, K.; Ramamurthi, K. Chemical Spray Pyrolysis Deposition of Transparent and Conducting Fe Doped CdO Thin Films for Ethanol Sensor. *Mater. Sci. Semicond. Process.* **2015**, *40*, 879–884.
- (29) Wang, B. J.; Ma, S. Y.; Pei, S. T.; Xu, X. L.; Cao, P. F.; Zhang, J. L.; Zhang, R.; Xu, X. H.; Han, T. High Specific Surface Area SnO2 Prepared by Calcining Sn-MOFs and Their Formaldehyde-Sensing Characteristics. *Sens. Actuators, B* **2020**, *321*, 128560.
- (30) Meng, D.; Liu, D.; Wang, G.; Shen, Y.; San, X.; Li, M.; Meng, F. Low-Temperature Formaldehyde Gas Sensors Based on NiO-SnO2 Heterojunction Microflowers Assembled by Thin Porous Nanosheets. Sens. Actuators, B 2018, 273, 418–428.
- (31) Wang, T.; Sun, P.; Liu, F.; Lu, G. Revealing the Correlation between Gas Selectivity and Semiconductor Energy Band Structure Derived from Off-Stoichiometric Spinel CdGa2O4. Sens. Actuators, B 2022, 352, 131039.
- (32) Velusamy, P.; Ramesh Babu, R.; Ramamurthi, K.; Elangovan, E.; Viegas, J. Effect of La Doping on the Structural, Optical and Electrical Properties of Spray Pyrolytically Deposited CdO Thin Films. J. Alloys Compd. 2017, 708, 804–812.
- (33) Velusamy, P.; Babu, R. R.; Ramamurthi, K.; Dahlem, M. S.; Elangovan, E. Highly Transparent Conducting Cerium Incorporated CdO Thin Films Deposited by a Spray Pyrolytic Technique. *RSC Adv.* **2015**, *5*, 102741–102749.
- (34) Velusamy, P.; Babu, R. R.; Ramamurthi, K.; Elangovan, E.; Viegas, J.; Dahlem, M. S.; Arivanandhan, M. Characterization of Spray Pyrolytically Deposited High Mobility Praseodymium Doped CdO Thin Films. *Ceram. Int.* **2016**, 42, 12675–12685.

- (35) Velusamy, P.; Xing, R.; Babu, R. R.; Elangovan, E.; Viegas, J.; Liu, S.; Sridharan, M. A Study on Formaldehyde Gas Sensing and Optoelectronic Properties of Bi-Doped CdO Thin Films Deposited by an Economic Solution Process. *Sens. Actuators, B* **2019**, 297, 126718.
- (36) Li, T.; Zeng, W.; Long, H.; Wang, Z. Nanosheet-assembled hierarchical SnO 2 nanostructures for efficient gas-sensing applications. *Sens. Actuators, B* **2016**, 231, 120–128.
- (37) Ji, H.; Zeng, W.; Li, Y. Gas Sensing Mechanisms of Metal Oxide Semiconductors: A Focus Review. *Nanoscale* **2019**, *11*, 22664–22684.
- (38) Das, S.; Mojumder, S.; Saha, D.; Pal, M. Influence of Major Parameters on the Sensing Mechanism of Semiconductor Metal Oxide Based Chemiresistive Gas Sensors: A Review Focused on Personalized Healthcare. Sens. Actuators, B 2022, 352, 131066.
- (39) Ran, Y.; Li, Y.; Cui, X.; Lai, T.; Yao, L.; Zhao, R.; Wang, L.; Wang, Y. Sm-Doped SnO2 Nanoparticles Synthesized via Solvothermal Method as a High-Performance Formaldehyde Sensing Material for Gas Sensors. *J. Mater. Sci.: Mater. Electron.* **2021**, 32, 8249–8264.
- (40) Yang, W.; Prabhakar, R. R.; Tan, J.; Tilley, S. D.; Moon, J. Strategies for Enhancing the Photocurrent, Photovoltage, and Stability of Photoelectrodes for Photoelectrochemical Water Splitting. *Chem. Soc. Rev.* **2019**, *48*, 4979–5015.
- (41) Yin, M.; Liu, S. Preparation of ZnO Hollow Spheres with Different Surface Roughness and Their Enhanced Gas Sensing Property. Sens. Actuators, B 2014, 197, 58–65.

□ Recommended by ACS

Controllable Vertical Nitrogen Doping in Nanoscaled Molybdenum Diselenide Films for Selective Sensing of NH₃ and NO₂ Gases

Kuangye Wang, Yu-Lun Chueh, et al.

APRIL 04, 2023

ACS APPLIED NANO MATERIALS

READ 🖸

Growth and Characterization of Sputtered ZnO:ZnGa₂O₄ Dual-Phase Films on Sapphire Substrates for NO Gas-Sensing Applications

Anoop Kumar Singh, Dong-Sing Wuu, et al.

MAY 08, 2023

ACS APPLIED ELECTRONIC MATERIALS

READ 🗹

Flame-Spray-Synthesized La₂O₃-Loaded WO₃ Nanoparticle Films for NO₂ Sensing

Mameaseng Siriwalai, Chaikarn Liewhiran, et al.

JANUARY 17, 2023

ACS APPLIED NANO MATERIALS

READ **C**

Highly Selective Room Temperature Detection of NH_3 and NO_x Using Oxygen-Deficient $W_{18}O_{49}$ -Supported WS_2 Heterojunctions

Mathankumar Manoharan, Ramasamy Thangavelu Rajendra Kumar, et al. JANUARY 13, 2023

ACS APPLIED MATERIALS & INTERFACES

READ 🗹

Get More Suggestions >